PG
Petroleum Geoscience

Research article

Published Online First

doi:10.1144/petgeo2015-017

Petrophysical and numerical seismic modelling of CO_2 geological storage in the E6 structure, Baltic Sea, offshore Latvia

Kazbulat Shogenov[1*], Davide Gei[2], Edy Forlin[2] & Alla Shogenova[1]

[1] Institute of Geology, Tallinn University of Technology, Ehitajate tee 5, Tallinn 19086, Estonia
[2] Istituto Nazionale di Oceanografia e di Geofisica Sperimentale (OGS), Borgo Grotta Gigante, 42/c, 34010 Sgonico Trieste, Italy
* Correspondence: kazbulat.shogenov@ttu.ee

Abstract: Time-lapse numerical seismic modelling based on rock physics studies was for the first time applied to analyse the feasibility of CO_2 storage monitoring in the largest Latvian offshore geological structure E6 in the Baltic Sea. The novelty of this approach was the coupling of the chemically induced petrophysical alteration effect of CO_2-hosting rocks measured in laboratory with time-lapse numerical seismic modelling. Synthetic seismograms were computed for the E6 structure, where the sandstone reservoir of the Deimena Formation of Cambrian Series 3 (earlier Middle Cambrian) was saturated with different concentrations of CO_2. The synthetic seismograms obtained after CO_2 injection were compared with the baseline. The following four scenarios were considered: (1) a uniform model without the alteration effect; (2) a uniform model with the alteration effect; (3) a plume model without the alteration effect; and (4) a plume model with the alteration effect.

The presence of CO_2 in the reservoir layers can be detected by direct comparison and interpretation of plane-wave synthetic seismic sections, and is clearly observed when one displays the difference between the baseline and post-CO_2 injection synthetics. The normalized root-mean-square imaging techniques also clearly highlight the time-lapse differences between the baseline and post-injection seismic data.

The laboratory-conducted alteration of the petrophysical properties of the reservoir had a strong influence on the reflected signals in the seismic sections. The greatest difference was revealed on seismic sections with 1% CO_2 saturation, increasing the detectability of the stored CO_2. The difference decreased with an increase in CO_2 content.

The saturation of CO_2 could be qualitatively estimated up to a value of 5%. Higher saturation produced a strong signal in the repeatability metrics but the seismic velocity varied so slightly with the increasing gas content that the estimation was challenging. A time shift or push-down of the reflectors below the CO_2 storage area was observed for all scenarios.

According to changes in the amplitude and two-way travel times in the presence of CO_2, reflection seismics could detect CO_2 injected into the deep aquifer formations even with low CO_2 saturation values.

Our data showed the effectiveness of the implemented time-lapse rock physics and seismic methods in the monitoring of the CO_2 plume evolution and migration in the E6 offshore oil-bearing structure. The new results obtained could be applied to other prospective structures in the Baltic region.

Received 6 March 2015; **revised** 12 November 2015; **accepted** 4 December 2015

Introduction

Carbon dioxide (CO_2) is an important greenhouse gas responsible for recent global climate change. It is capable of absorbing the heat radiation from the Earth's surface and contributes to the increase in atmospheric temperature. If the level of CO_2 in the atmosphere changes drastically, the greenhouse effect may alter the conditions on the planet (National Research Council 2010). Many organizations – for example, the Intergovernmental Panel on Climate Change (IPCC 2005) and the United States Environmental Protection Agency (USEPA 2013) – have stated that fossil fuel combustion is a major source of CO_2 emissions to the atmosphere (United States Geological Survey Geologic Carbon Dioxide Storage Resources Assessment Team 2013). Our previous studies have shown that the Estonian power plants emit more CO_2 than the energy sector of two other Baltic countries (Latvia and Lithuania) put together. Estonian CO_2 emissions per capita are among the highest in Europe and in the world owing to the use of local oil shale for energy production (e.g. Shogenova *et al*. 2009*a*, *b*, 2011*a*, *b*).

Carbon capture and storage (CCS) is one of the most effective measures for capturing and trapping CO_2, and plays an essential role in reducing the greenhouse effect and mitigating the climate change on our planet (IEA 2004, 2013; Holloway 2005; IPCC 2005, 2013; Bachu *et al*. 2007; Arts *et al*. 2008). The overall reduction of CO_2 emissions is likely to involve some combination of technologies. For the immediate future, however, the storage of industrial CO_2 emissions in geological reservoirs (CGS) is a prospective technology because the knowledge derived from the oil and gas production industries has helped to solve some of the major engineering challenges.

The Estonian territory is unsuitable for CGS because of its geological setting (i.e., shallow sedimentary basin and potable water available in all known aquifers). The most prospective structures for CGS in the East Baltic region (Estonia, Latvia and Lithuania) are located in Latvia, and consist of a number of onshore and offshore anticlines (Sliaupa *et al*. 2008; Shogenova *et al*. 2009*a*, *b*, 2011*a*, *b*; Shogenov *et al*. 2013*a*, *b*; Šliaupa *et al*. 2013).

In this research, we focus on a coupled petrophysical and numerical seismic modelling methodology to study the feasibility of monitoring CGS in the Latvian offshore deep geological structure E6, which is oil-bearing in the Saldus Formation of the Upper Ordovician secondary cap rock. It was selected as one of the most prospective structures in the Latvian area of the Baltic region in our earlier published studies (Fig. 1) (Shogenov *et al*. 2013*a*, *b*).

The E6 structure is located in the Baltic Sea, 37 km from the coast of Latvia. Its estimated conservative and optimistic CO_2 storage capacity (160–400 Mt, respectively) makes it the largest among all the studied onshore and offshore structures in the Baltic

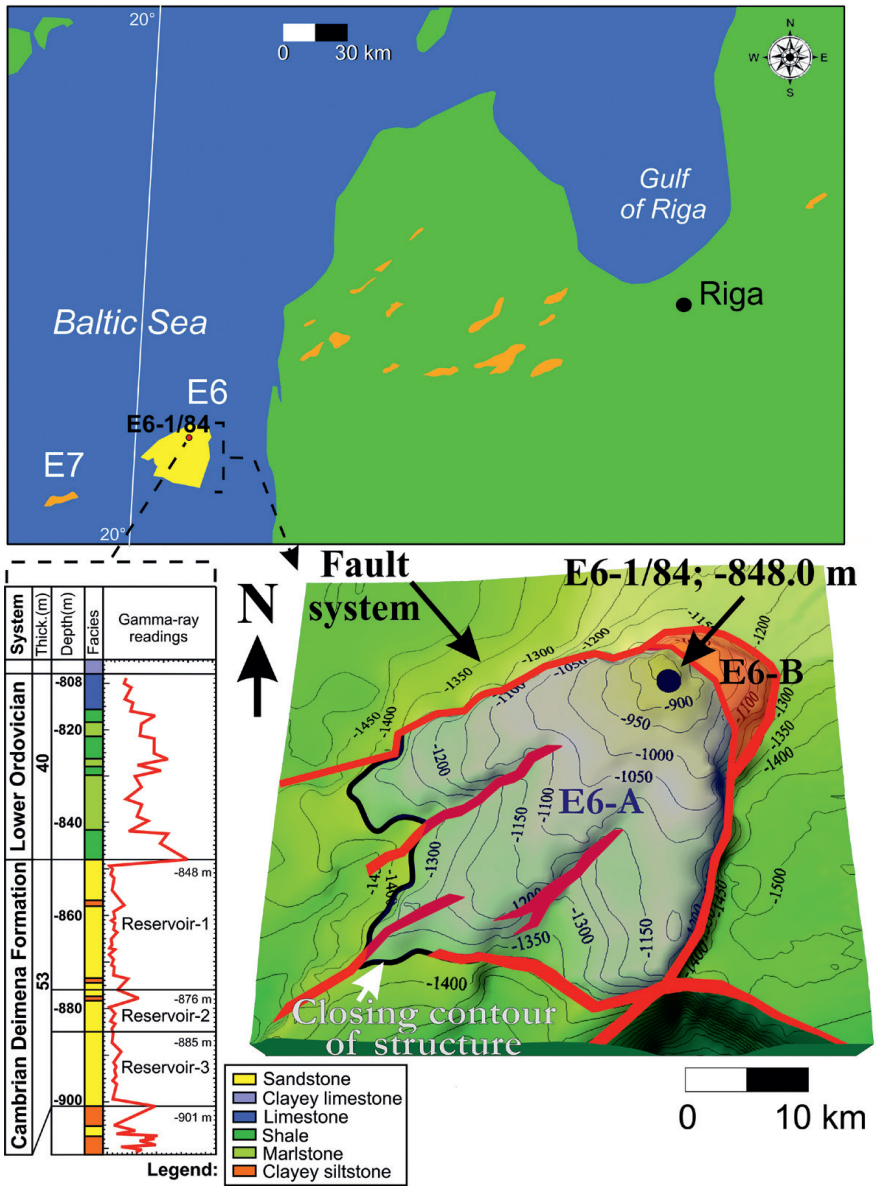

Fig. 1. Locations of Latvian onshore structures and the E7 structure offshore Lithuania (orange) prospective site for CGS (CO_2 storage potential exceeding 2 Mt) in the Cambrian aquifer, and the studied E6 structure offshore Latvia (yellow), with the location of the well, lithological cross-section and gamma-ray logging data, and the 3D geological model of the top of the Cambrian Deimena Formation of the E6 structure (modified after Shogenov *et al*. 2013*b*).

region (Shogenov *et al*. 2013*a*, *b*). The prospective reservoir for CGS is the Deimena Formation of Cambrian Series 3 (earlier Middle Cambrian) (848–901 m depth in well E6-1/84) composed of dark- and light-grey, fine-grained, loosely and medium-cemented, oil-impregnated sandstones. Oil impregnation ranges from weak irregular to strong regular (Shogenov *et al*. 2013*b*). A new classification of reservoir rock quality for CO_2 storage based on permeability and porosity was proposed in our recent study (Shogenov *et al*. 2015*b*). According to this classification, the reservoir rocks from the E6 structure are represented mostly by sandstones of 'good' reservoir quality belonging to class III 'appropriate' for CGS (permeability 100–300 mD and porosity >18%). These sandstones are interbedded with sandstones of 'cautionary-2' reservoir quality related to 'cautionary' for CGS rocks (permeability 10–100 mD and porosity 7–18%). In this study, we did not consider oil impregnation of the reservoir rocks because of their very low saturation. The structure is an anticline fold bounded by faults on three sides. The total area of the structure is 600 km^2 and the closing contour line (or spill point) of the reservoir is located at a depth of 1350 m below sea level (bsl). These parameters were interpreted by Shogenov *et al*. (2013*b*), using structural maps of the study area and an available seismic profile. The previous closing contour line, earlier reported by the Latvian Environmental, Geology and Meteorology Centre (LEGMC), was at 950 m bsl.

An inner fault divides the E6 structure into two different compartments (E6-A and E6-B) (Fig. 1). Shogenov *et al*. (2013*b*) assumed that the fault separates these compartments, preventing the migration of CO_2 from one compartment to the other during injection. In the case of CO_2 storage, an additional well should be drilled in part E6-B.

The approximate area of the larger compartment (E6-A) is 553 km^2, while the smaller one (E6-B) takes up 47 km^2. The Deimena reservoir in well E6-1/84 is a 53 m-thick aquifer at a depth of 848 m bsl (the top of the Deimena Formation), with a water salinity of 99 000 ppm (98.89 $g\,l^{-1}$).

Modelling was carried out for the larger part, E6-A. The top of the Cambrian Deimena Formation sandstone reservoir, located at a depth of 848 m bsl, is unconformably covered by a 40 m-thick Lower Ordovician clayey primary cap rock. Secondary cap rocks are represented by Ordovician and Silurian clayey carbonate rocks, and are covered by Devonian siliciclastic

Table 1. *Physical parameters of the main layers shown in the model (Fig. 2)*

Layer	Lithology	Depth* (m)	T (°C)	P (MPa)	ρ_{wet} (kg m^{-3})	φ (%)	κ (mD)	V_P (m s^{-1})	V_S (m s^{-1})	Q_P	Q_S	M (GPa)	K_{dry} (GPa)
Seawater	–	0	10	0.1	1030	–	–	1480	–	–	–	–	–
Devonian	Sandstone	36.5	7	0.8	2226	15	2	2474	1133	66	18	2.86	–
Silurian	Carbonate shales	580	31	6.3	2244	6–16	<0.1	2570	1043	71	16	2.44	–
Ordovician Saldus Formation (oil reservoir)	Limestone	702	35	8.4	2342	18	6	2970	1395	95	28	4.56	–
Ordovician (cap rock)	Carbonate shales	712.5	35	8.6	2540	3	<0.01	2628	1093	74	17	3.04	–
Deimena (Reservoir-1)	Sandstone	848	37	9.3	2341	21	160	2836	1400	250	94	4.59	4.21
Deimena (Reservoir-2)	Sandstone	876	37	9.7	2400	17	60	2873	1349	761	255	4.37	4.00
Deimena (Reservoir-3)	Sandstone	885	37	9.8	2306	25	230	2872	1510	211	87	5.26	4.82
Cambrian	Siltstone	901	38	10	2324	3–18	0.2–23	2746	1675	81	40	6.52	–
Basement	Granite	1029	41	11.2	2675	–	–	5800	3454	362	171	31.9	–

*Depth of the top of the formation in well E6-1/84
All formations, except for the oil reservoir, are saturated with brine. Temperature (T) and pressure (P) of the formations top; ρ_{wet}, bulk density of brine-saturated rock samples; φ, effective porosity; κ, permeability; V_P and V_S, velocities of compressional (P) and shear (S) waves, respectively; Q_P and Q_S, quality factors of P- and S-waves, respectively; μ and K_{dry}, shear and bulk modules of dry rocks, respectively (K_{dry} is only estimated for reservoir formations).

and carbonate rocks (Table 1). A small oil deposit is found in the limestones of the Upper Ordovician Saldus Formation (10.5 m; Shogenov *et al*. 2013*a*, *b*). The bottom of the Deimena Formation is underlain by 117 m-thick argillaceous siltstones, sandstones and claystones of the Cambrian Kybartai, Rausve, Vergale and Talsi formations, and 11 m of Ediacaran tuffaceous sediments. These rocks overlie Palaeoproterozoic gneissose granites at a depth of 1029 m bsl in well E6-1/84 (Grigelis 2011; Shogenov *et al*. 2013*a*, *b*).

The time-lapse seismic method

The time-lapse seismic method is known as a highly suitable technique for monitoring the CO_2 injection into a saline aquifer (Arts *et al*. 2004*a*, *b*, 2008; Chadwick *et al*. 2008). Generally, the effects of CO_2 on seismic data are large both in terms of seismic amplitudes and observed velocity push-down (Arts *et al*. 2000). In this research, we have applied a time-lapse rock physics and numerical seismic modelling method (Carcione 2007) to compute synthetic seismograms before and after CO_2 injection into the E6 structure, and to provide the basis for further CGS monitoring plan in the study area. This methodology permits the prediction of the seismic response of CO_2 in the storage site, planning for the monitoring of plume migration, estimation of the integrity of the reservoir and supports notification of possible leakage. It also allows optimization of the seismic surveys, which should be repeated over time to monitor the evolution of injected CO_2 (Rossi *et al*. 2008; Picotti *et al*. 2012).

A large number of cognate studies have been carried out over several recent years looking at operating CO_2 storage sites (e.g. the Sleipner in Norway: Arts *et al*. 2003, 2004*a*, *b*; Carcione *et al*. 2006; Chadwick *et al*. 2006) and the potential for CGS sites (e.g. Atzbach-Schwanenstadt in Austria: Rossi *et al*. 2008; Picotti *et al*. 2012; and Calgary in Canada: Vera 2012). These studies have given similar results: (1) CO_2 injected into the geological storage site can be detected by time-lapse seismic surveys even with low CO_2 saturation values; (2) P-wave velocity drops quickly as CO_2 saturation in the reservoir increases from 0 to 20%, with a slight increase in velocity at higher saturations; (3) the magnitude of the change in S-wave velocity is very small in comparison with variations in the P-wave velocity; (4) the presence of the CO_2 plume can be detected by direct interpretation of seismic sections in the injection zone, but more effectively by determining the difference between the baseline (seismic survey acquired before CO_2 injection) and repeated surveys or by considering more sophisticated repeatability metrics such as the normalized root-mean-square (NRMS) technique. These techniques are extremely sensitive to imaging the smallest changes between the seismic baseline and repeated seismic sections data (Kragh & Christie 2002), and were used to compare seismic datasets before and after CO_2 injection, simulating seismic acquisitions at different times over the same study area.

Shogenov *et al*. (2015*a*, *b*) performed a CO_2-injection-like storage experiment simulated in the laboratory, and studied petrophysical alterations in the reservoir rocks caused by geochemical and mineralogical CO_2–fluid–rock interactions. In the present study, for the first time according to our knowledge, the petrophysical alteration effect induced by CO_2 was incorporated into the numerical seismic modelling methodology. Petrophysical properties of the host rocks, measured before and after the alteration experiment, were applied in modelling. The 'alteration approach' indicated the importance of implementing this effect in such a modelling routine for CGS monitoring and filled the gap in previous seismic models (Pawar *et al*. 2006).

A uniform model without the alteration effect of the offshore oil-bearing structure E6 from the Baltic Sea was presented in Shogenov & Gei (2013). In this paper, we have updated some properties implemented in the previous study with data from the petrophysical alteration analysis.

Data and methods

Two different approaches to CO_2 distribution in the host rock were applied in numerical seismic modelling: (i) homogeneous CO_2 saturation of the reservoir (the uniform model); and (ii) CO_2 plume accumulation (the plume model). For this reason, we produced synthetic datasets for four scenarios: (1) a uniform model without the alteration effect; (2) a uniform model with the alteration effect; (3) a plume model without the alteration effect; and (4) a plume model with the alteration effect. Synthetic seismic sections were produced, analysed and compared with the baseline dataset (before the injection of CO_2). We considered the first two scenarios in order to explore the effectiveness of the seismic technique for CGS monitoring in the long term, when CO_2 has homogeneously spread within the storage reservoir. The third and fourth scenarios present approaches that are more realistic in the short term, and involve modelling that is more complex (plume shape and inhomogeneous CO_2 saturation).

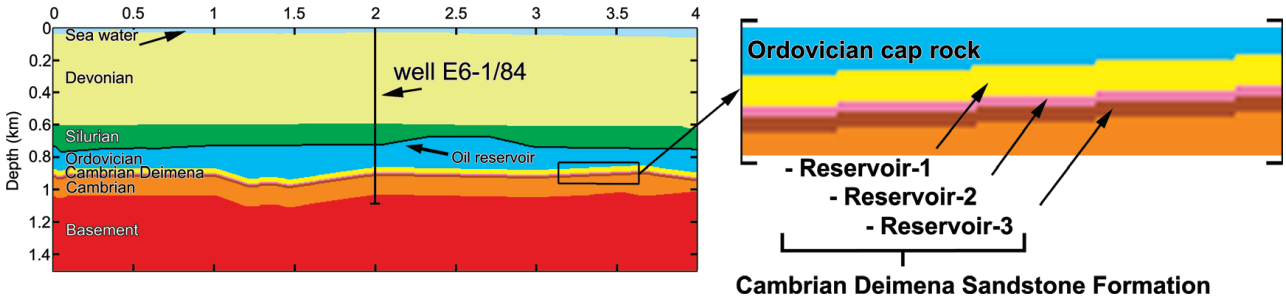

Fig. 2. Two-dimensional geological model of the E6 offshore structure implemented for seismic modelling and a magnification of the three reservoirs (modified after Shogenov & Gei 2013).

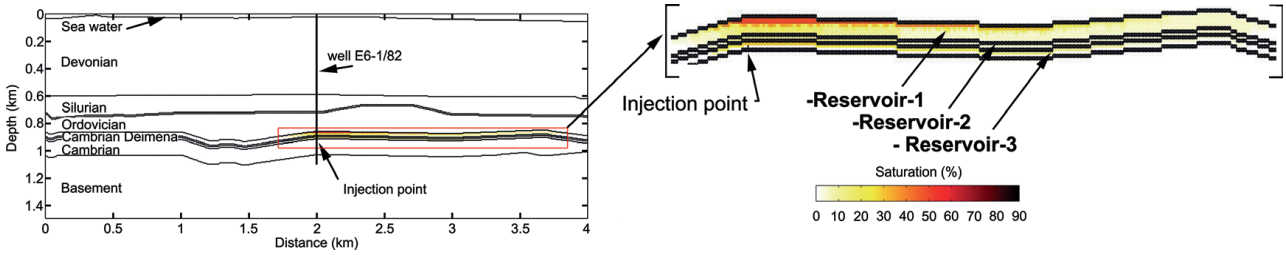

Fig. 3. Plume saturation model of CO_2 injected into the reservoir formation in the E6 structure. Different saturations of CO_2 and reservoir formation fluids are indicated. Black lines within the structure are formation contacts.

2D uniform modelling

Figure 2 shows the 2D geological model implemented for the numerical seismic modelling and extrapolated for the interpretation of the E6 seismic section. Well E6-1/84 is located approximately in the middle of the model. According to specific petrophysical properties, the Deimena reservoir was split into three parts: Reservoir-1, Reservoir-2 and Reservoir-3. Owing to the shortage of experimental data (only one well was drilled in the structure), the three subreservoirs were simplified to be homogeneous without vertical or lateral heterogeneity. The Saldus Formation of the Upper Ordovician oil reservoir is shown by a 10 m-thick black layer between the Ordovician and the Silurian (Fig. 2).

All the layers in the geological model were characterized and populated with specific lithology, and measured or computed petrophysical properties were recalculated under *in situ* conditions before and after the alteration experiment (Table 1). The 11 m-thick Ediacaran tuffaceous sediments were not considered in modelling due to the absence of measured physical properties.

CO_2 plume modelling

A simplified CO_2 plume accumulation model was based on studies of gravity flows within a permeable medium for an axisymmetric geometry (Huppert & Woods 1995; Lyle *et al*. 2005; Bickle *et al*. 2007), and it took field monitoring and numerical modelling studies of the existing offshore storage site (Sleipner, North Sea: e.g. Fornel & Estublier 2013; Zhang & Agarwal 2014) into account. The possible evolution and migration of the CO_2 plume within the reservoir layers in the E6 potential storage site was described at a specific time and with a given amount of injected CO_2. The fluid saturation has been assumed according to the structural, stratigraphic, lithological and petrophysical properties of different reservoir layers (Scenario 3 and Scenario 4: Fig. 3).

Seismic and poro-viscoelastic properties

The seismic parameters of the reservoir layers were computed using properties of rocks – grain and dry-rock density (ρ_{solid} and ρ_{dry}, respectively), effective porosity and permeability (φ and κ, respectively), and P-wave velocity (V_{Pdry}) – measured on dry-rock samples before and after the alteration experiments at the IFP Energies nouvelles (IFPEN) rock physics laboratories (Shogenov *et al*. 2013*a*, *b*, 2015*a*, *b*; Shogenov & Gei 2013). The measured parameters were coupled with data available from the exploration report for the E6 structure (Andrushenko *et al*. 1985). The measurement results from the IFPEN laboratories, data from the report or estimated data (average of the measurement data and those reported in Andrushenko *et al*. (1985) for different parts of the reservoir layer) were applied in modelling. The estimated ρ_{solid} value was used for Reservoir-1, that from the exploration report for Reservoir-2 and the measured value for Reservoir-3. Estimated ρ_{dry}, φ and κ were employed for Reservoir-1 and Reservoir-3, and data from the exploration report for Reservoir-2. Estimated V_{Pdry} was used for Reservoir-1, and the value from the exploration report for Reservoir-2 and Reservoir-3 (Table 1).

The results of the petrophysical changes of the E6 structure for Reservoir-1 and Reservoir-3 were considered as reservoir rock properties after the alteration experiment (Shogenov *et al*. 2015*a*, *b*). Owing to the lack of samples characterizing the change in the properties of the rock in Reservoir-2, and the V_{Pdry} change in Reservoir-1 and Reservoir-3, alteration results for equivalent reservoir samples (with similar properties before alteration) from the Lithuanian offshore E7 structure were used (Fig. 1) (Shogenov *et al*. 2013*b*, 2015*a*, *b*).

Experimental P-wave velocities (V_{Pwet}) obtained from unpublished results of active seismic surveys, laboratory measurements of dry and wet samples of the oil reservoir of the Upper Ordovician Saldus Formation from well E6-1/84 (Andrushenko *et al*. 1985), and measurements of more than 1000 rock samples from the northern part of the Baltic sedimentary basin (Shogenova *et al*. 2010) were assigned to the layers above and below the storage formation.

Seismic properties of different formations (Tables 1 & 2) (Shogenov & Gei 2013) were computed with consideration to the rock physics theories described in the following sections.

Reservoir formation

The velocity and attenuation of compressional seismic waves for the reservoir rocks partially saturated with carbon dioxide were

computed following White's mesoscopic rock physics theory (White 1975). A detailed review of White's theory can be found in Carcione *et al*. (2006) or Picotti *et al*. (2012). This model of attenuation gives realistic seismic properties (P-wave velocity and quality factor) when dry-rock moduli, porosity, bulk density, permeability, fluid saturation and the dominant frequency of the seismic signal are provided. The saturation is assumed to be patchy, considering that spherical gas pockets are much larger than solid grains of the sediment, but much smaller than the wavelength (White 1975; Carcione *et al*. 2003, 2006, 2012; Carcione 2007).

We applied a fluid-substitution procedure to compute the seismic properties of brine-saturated rocks and the same rocks partially saturated with CO_2. Physical properties of the saturating fluids are needed for modelling. The seismic velocity and density of brine were computed under *in situ* conditions using the empirical relationships of Batzle & Wang (1992). The compressibility and density of CO_2 at *in situ* pressure and temperature were computed with the Peng–Robinson equation of state (Peng & Robinson 1976; Picotti *et al*. 2012).

Assuming that the Poisson's ratio (v) for unconsolidated sands is equal to 0.1 (Gregory 1977), the S-wave velocity of dry rocks (V_{Sdry}) can be computed using the relationship provided by White (1965) and Castagna *et al*. (1985):

$$V_{Sdry} = \frac{V_{Pdry}}{1.5}. \quad (1)$$

The shear modulus, μ, and the bulk modulus of dry rock, K_{dry}, are computed from:

$$\mu = V_{Sdry}^2 \rho_{dry} \quad (2)$$

and

$$K_{dry} = V_{Pdry}^2 \rho_{dry} - \frac{4}{3}\mu. \quad (3)$$

Owing to the thermodynamic restrictions, the shear and bulk moduli acquire positive values (Gercek 2007). The Poisson's ratio, v, varies between 0 and 0.5, and a value of 0.25 is often assumed (De Waals 1986). The value of v can be found by the equation (e.g. Bacon *et al*. 2003):

$$\nu = 0.5\frac{3K - 2\mu}{2\mu + 6K}. \quad (4)$$

The Poisson's ratio of wet sandstones of the E6 structure, v_{wet} (Reservoir-1, Reservoir-2 and Reservoir-3), before and after alteration is between 0.31 and 0.37, within the range of values reported by Gercek (2007) (from 0.4 for unconsolidated sands to values well below 0.05 for tight rocks).

The density of the partially saturated rock is obtained using the formula:

$$\rho_{wet} = \rho_{solid}(1 - \varphi/100) + \rho_{fluid}\varphi/100 \quad (5)$$

where ρ_{fluid} is the density of the gas–brine mixture:

$$\rho_{fluid} = \rho_{brine} s_{brine} + \rho_{gas} s_{gas} \quad (6)$$

where s_{brine} and s_{gas} are relative saturations, such that $s_{brine}+s_{gas}=1$.

The S-wave velocities of partially saturated reservoir rocks are computed using the formula:

$$V_{Swet} = \sqrt{\mu/\rho_{wet}}. \quad (7)$$

Since White's theory does not predict any shear dissipation, we describe attenuation with a Zener element according to the theory presented in Carcione *et al*. (2012).

Other formations

As mentioned previously, properties of the cap rock and underlying layers of the E6 structure (Table 1) were obtained from the exploration report by Andrushenko *et al*. (1985), when available. The missing parameters were estimated by the empirical relationships offered by Ludwig *et al*. (1970), Castagna *et al*. (1985, 1993), Saxena (2004) and Brocher (2005) for different rock types, as described below.

Average V_{Swet} (in $m\,s^{-1}$) for the Devonian sandstone formation was estimated using reported V_{Pwet} (in $m\,s^{-1}$) values for Devonian sandstone (Andrushenko *et al*. 1985) and an empirical equation derived from laboratory V_P/V_S data for water-saturated sandstones (Castagna *et al*. 1993):

$$V_{Swet} = 0.804\,V_{Pwet} - 856. \quad (8)$$

The ρ_{wet} value for the Devonian sandstones was found using equation (5), reported averages were used for ρ_{solid} (Shogenova *et al*. 2010) and φ (Andrushenko *et al*. 1985), and ρ_{brine} was computed under *in situ* conditions using the empirical relationships of Batzle & Wang (1992).

Average V_{Swet} values (in $m\,s^{-1}$) for the Silurian and Ordovician cap rocks (claystones and shales) were estimated using reported V_{Pwet} (in $m\,s^{-1}$) (Andrushenko *et al*. 1985) and the well-known *in situ* 'mudrock line', obtained from relationships for shales by Castagna *et al*. (1985):

$$V_{Swet} = 0.862\,V_{Pwet} - 1172. \quad (9)$$

The ρ_{wet} of the Silurian cap rock layer was estimated using polynomial and power-law forms of the velocity–density relationship by Gardner *et al*. (1974), presented in Castagna *et al*. (1993):

$$\rho_{wet(shales)} = -0.0261\,V_{Pwet}^2 + 0.373\,V_{Pwet} + 1.458. \quad (10)$$

Units are $km\,s^{-1}$ and $g\,cm^{-3}$ for velocity and density, respectively.

The ρ_{wet} of the Ordovician cap rock layer was calculated using equation (5). Rock physical properties (ρ_{solid} and φ) were derived from the laboratory data of Andrushenko *et al*. (1985).

The V_{Swet} of the Ordovician limestone oil reservoir was estimated using equation (7), using μ obtained from equation (2) and ρ_{wet} using equation (5). V_{Pdry}, V_{Pwet}, ρ_{dry}, ρ_{solid}, ρ_{fluid} (oil) and φ were derived from the laboratory data of Andrushenko *et al*. (1985). V_{Sdry}, necessary for the calculation of μ, was derived using the V_{Pdry}–V_{Sdry} theoretical relationship for dry limestones (Saxena 2004):

$$V_{Sdry} = \frac{V_{Pdry}}{1.8}. \quad (11)$$

Average V_{Sdry}, μ and V_{Swet} values for the Cambrian siltstone layer, underlying the reservoir, were estimated using equations (1), (2) and (7), respectively, and ρ_{wet}, ρ_{dry} and V_{Pdry} were derived from laboratory measurement data available in Shogenova *et al*. (2010). The V_{Pwet} value was taken from the report on well E6-1/84 by Andrushenko *et al*. (1985).

The V_{Pwet} value for the basement layer was derived from an average of laboratory data for more than 4000 water-saturated basement samples from the drill cores of the Kola Peninsula (Baltic Shield), Ukraine, Caucasus, Urals, Kazakhstan, Transbaikal and Primorsky Krai (Dortman 1992). An average value of V_{Swet} (in $km\,s^{-1}$) for the basement was estimated from V_{Pwet} (in $km\,s^{-1}$) using a 'Brocher's regression fit' (Brocher 2005):

$$V_{Swet} = 0.7858 - 1.2344\,V_{Pwet} + 0.7949\,V_{Pwet}^2 - 0.1238\,V_{Pwet}^3 + 0.0064\,V_{Pwet}^4. \quad (12)$$

The ρ_{wet} (in g cm^{-3}) of the basement layer was derived using the Nafe–Drake relationship in the 'Nafe–Drake curve', published by Ludwig *et al*. (1970) for a wide variety of sedimentary and crystalline rock types (for compressional wave velocities of between 1.5 and 6.1 km s^{-1}):

$$\rho_{wet} = 1.6612\,V_{Pwet} - 0.4721\,V_{Pwet}^2 + 0.0671\,V_{Pwet}^3 - 0.0043\,V_{Pwet}^4 + 0.000106\,V_{Pwet}^5. \quad (13)$$

The quality factors (Q) of all the formations, except for the reservoir, were computed from V_{Pwet} and V_{Swet} by empirical relationships proposed by Waters (1978) and Udias (1999), and also given in Haase & Stewart (2004):

$$1/Q_P = \left(\frac{\text{const.}}{V_P}\right)^2 \quad (14)$$

where Q_P is a the P-wave quality factor and const. is approximately 10^3, and:

$$Q_S = Q_P \frac{4}{3}\left(\frac{V_S}{V_P}\right)^2 \quad (15)$$

where Q_S is the S-wave quality factor.

Numerical seismic modelling

For numerical seismic modelling we considered the 2D viscoelastic wave equation, which was solved using a fourth-order Runge–Kutta time-stepping scheme and the staggered Fourier method to compute the spatial derivatives. This method is noise-free in the dynamic range, where regular grids generate artefacts that may have amplitudes similar to those of physical arrivals (Carcione 2007; Picotti *et al*. 2012).

The seismic simulations were performed over a numerical mesh obtained by discretizing the geological model given in Figure 2. A mesh of 240 000 (800×300) points with a grid point spacing of 5 m was built. We considered plane-wave simulations, approximating non-migrated zero offset sections, by simultaneously triggering sources located in each grid point of the upper edge of the numerical mesh. This procedure produces a plane wave propagating downwards. Every time the plane wave impinges on the interface between two different formations, it is reflected back to the upper edge of the geological model, coinciding with the sea surface, where the seismic wave field is recorded at each grid point. We computed synthetic seismograms of the baseline and after CO_2 injection, taking into consideration the homogeneous and plume gas distributions into the reservoir. Specific repeatability metrics – 'Difference' and NRMS sections of 4D seismic data – were used to qualitatively estimate changes in seismic reflections and to indicate differences, such as phase shifts and amplitude variations in time-lapse datasets (Kragh & Christie 2002; MacBeth *et al*. 2006; Vedanti *et al*. 2009; Lacombe *et al*. 2011; Picotti *et al*. 2012). In the case of CO_2 geological storage, the main differences in pre- and post-injection datasets are due to the different travel times (and amplitudes) of the reflectors affected by the presence of the gas. Travel times depend on velocity and, if the seismic velocity shows small variations with increasing CO_2 saturation, then the difference and NRMS sections will equally show small differences. The source time history is that of a Ricker wavelet with a dominant frequency of 35 Hz. Absorbing boundary conditions are implemented in absorbing strips of 40 grid point lengths, located at the bottom and sides of the numerical mesh to damp the wraparound phases.

Results

Seismic properties of the reservoir formations

The bulk density ρ_{wet} decreases over the whole range of CO_2 saturation. It is accompanied by a steep drop in V_{Pwet} and acoustic impedance in the range 1–10% CO_2 saturation, calculated for the reservoir rocks using the fluid substitution method (Table 3). Moreover, the mesoscopic attenuation shows a peak at about 5% CO_2 saturation in the reservoir rocks in all reservoir layers (Reservoir-1, Reservoir-2 and Reservoir-3), with minor differences between the scenarios with and without a petrophysical alteration effect. The decrease in P-wave velocity becomes insignificant in the range 10–50% CO_2 saturation. After 50% CO_2 saturation, V_{Pwet} starts to increase. V_{Swet} slightly increases from very low CO_2 saturations: this is due to a decrease in bulk density, as the shear modulus of the rock is not affected by the substitution of fluid (e.g. Kazemeini *et al*. 2010). The P-wave velocity drop in altered rocks (Scenario 2 and Scenario 4: Tables 1–3) is slightly higher than that in the non-altered rocks (Scenario 1 and Scenario 3: Tables 1–3). Figure 4 shows the bulk density, velocities, acoustic impedance and attenuation of Reservoir-1 as a function of CO_2 saturation for the original (initial) and altered core samples.

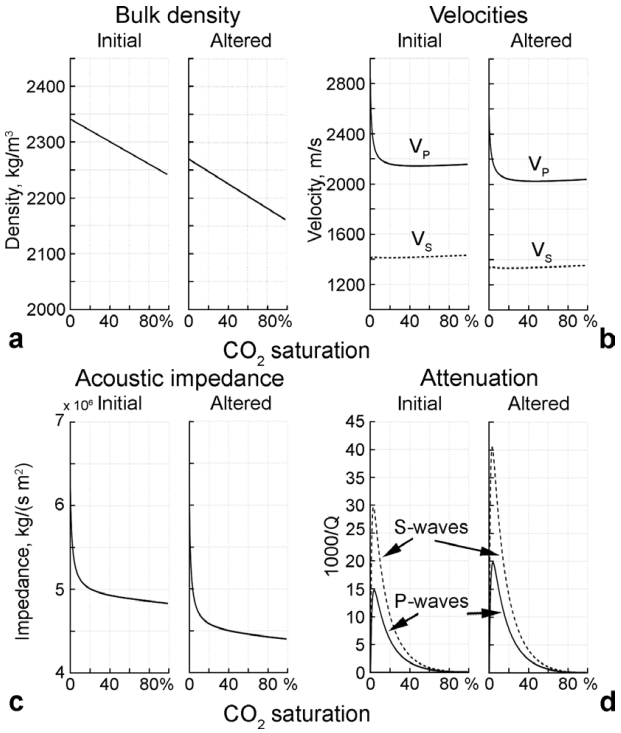

Fig. 4. (**a**) Bulk density, (**b**) P- and S-wave velocities (V_P and V_S, respectively), (**c**) acoustic impedance and (**d**) P- and S-wave attenuation ($1000/Q$) in the uppermost layer of the reservoir formation (Reservoir-1) of the Cambrian Deimena Formation sandstones v. CO_2 saturation in the initial state before the injection of CO_2 (without the alteration effect) and under altered conditions.

Synthetic seismic sections

Plane-wave datasets

The baseline synthetic plane-wave seismic section of the E6 offshore structure before CO_2 injection (Fig. 5a) was produced and compared with six synthetic seismic sections, reproducing different CO_2 saturation levels (1, 5, 10, 15, 50 and 90%) for the Deimena Formation, bearing in mind homogeneous gas saturation (Scenario 1: Fig. 5sc1-a). Repeated seismic simulations took the chemically induced petrophysical alteration effect of the reservoir rocks into account (Scenario 2: Fig. 5sc2-a). Modelling provided seismic images of the CO_2 storage in the E6 offshore structure at different times over the same area. Plane-wave sections of the modelled CO_2 plume in the E6 structure without and with the

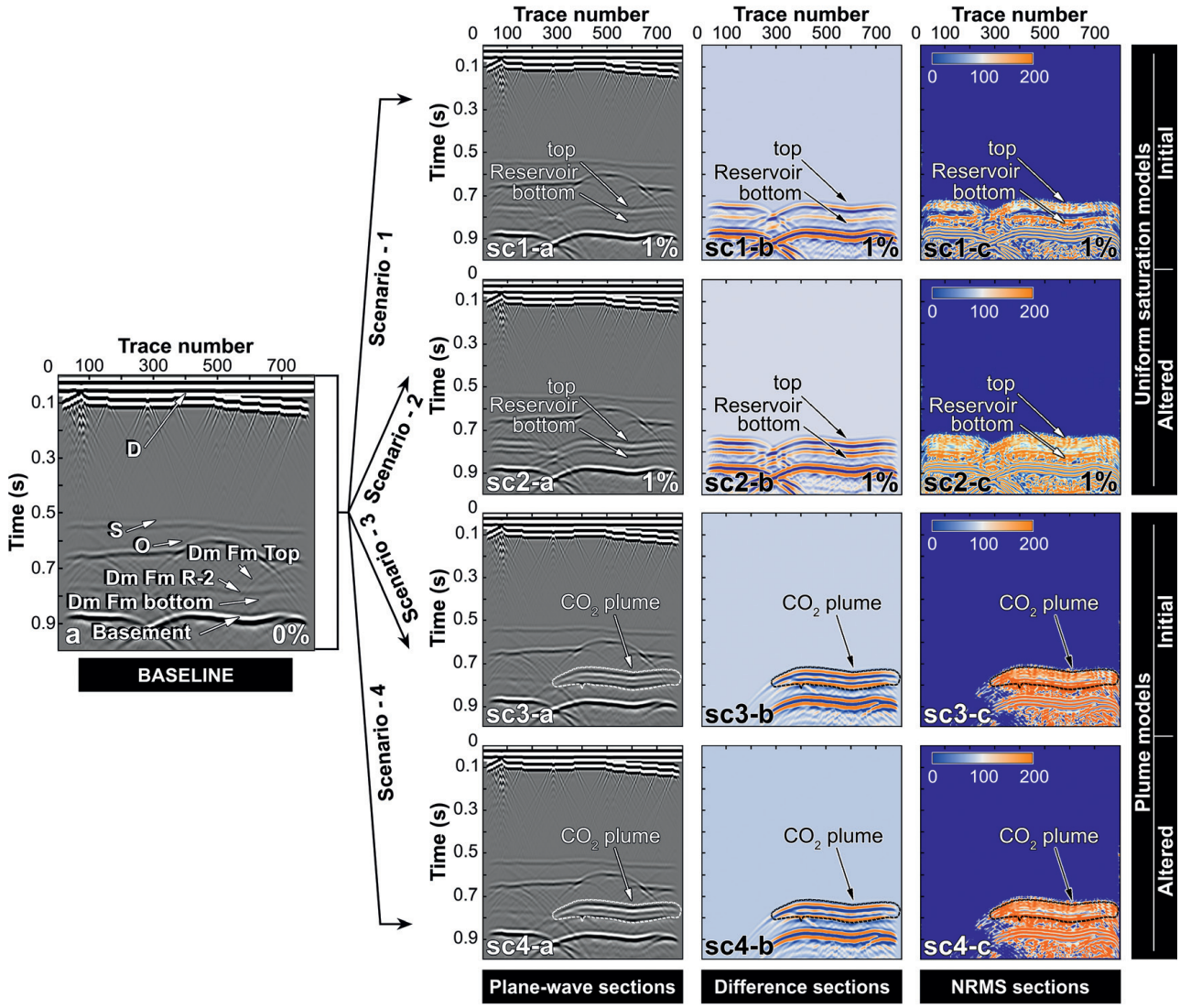

Fig. 5. (**a**) Baseline synthetic plane-wave section of the E6 structure, before the injection of CO_2. Reflectors of the tops of all the geological formations (D, Devonian; S, Silurian; O, Ordovician), the top and bottom of the Cambrian Deimena reservoir (Dm Fm), and the middle part of the Deimena Formation Reservoir-2 (Dm Fm R-2) are indicated: (**sc1-a**) plane-wave section of Scenario 1 (uniform model without the alteration effect) with 1% CO_2 saturation; 'Difference' (**sc1-b**) and NRMS (**sc1-c**) sections of the synthetic baseline and the seismic section of Scenario 1 with 1% CO_2; (**sc2-a–sc2-c**) seismic sections of Scenario 2 (uniform model with the alteration effect) with 1% CO_2 saturation; arrows indicate the top and bottom of the reservoir; (**sc3-a–sc3-c**) seismic sections of Scenario 3 (a plume model without the alteration effect); (**sc4-a–sc4-c**) seismic sections of Scenario 4 (a plume model with the alteration effect); arrows indicate the CO_2 plume.

petrophysical alteration effect were also computed (Scenario 3 (Fig. 5sc3-a) and Scenario 4 (Fig. 5sc4-a), respectively).

The presence of CO_2 in the reservoir layers could be detected by direct comparison and interpretation of the baseline and repeated synthetic surveys with different CO_2 saturation levels in Scenario 1 (Fig. 5sc1-a) and Scenario 2 (Fig. 5sc2-a), even from 1% saturation. The seismic reflections corresponding to the top and bottom of the three reservoirs became stronger with increasing CO_2 saturation, showing the best contrast up to 5% CO_2 saturation. The evolution of the reflection strength in the sections modelled beyond 5% CO_2 saturation was difficult to detect, as all synthetic plane-wave seismic sections in the range of 10–90% CO_2 saturation for a specific scenario were very similar.

A slight variation in time shift or velocity push-down was also detectable on the plane-wave plots for the layers below the reservoir formation. In 4D seismic surveys, the push-down anomaly, located below the plume volume, is a typical manifestation of the presence of a low-velocity fluid (e.g. CO_2) in the porous space, after displacement of the original pore fluid (e.g. brine) (Chadwick *et al*. 2008; Boait *et al*. 2012). The plane-wave sections of Scenario 3 (Fig. 5sc3-a) and Scenario 4 (Fig. 5sc4-a) clearly show the modelled CO_2 plume in the E6 storage site. Seismic reflections of the reservoir rocks with the petrophysical alteration effect (Scenario 2 and Scenario 4) showed higher reflectivity in all cases compared to Scenario 1 and Scenario 3.

'Difference' and NRMS sections

To monitor the presence of CO_2 within the storage site in more detail, the modelled numerical seismic baseline section of the E6 structure was compared with repeat synthetic sections at different CO_2 saturations. The 'Difference' and NRMS techniques were applied to each scenario (Fig. 5). In addition, in order to understand the effect of the alteration on the reflectivity of the reservoir, we compared each seismic line without and with petrophysical alteration (Fig. 6). Using 'Difference' and NRMS metrics, CO_2 was clearly visible from a low gas saturation (Fig. 5). However, for

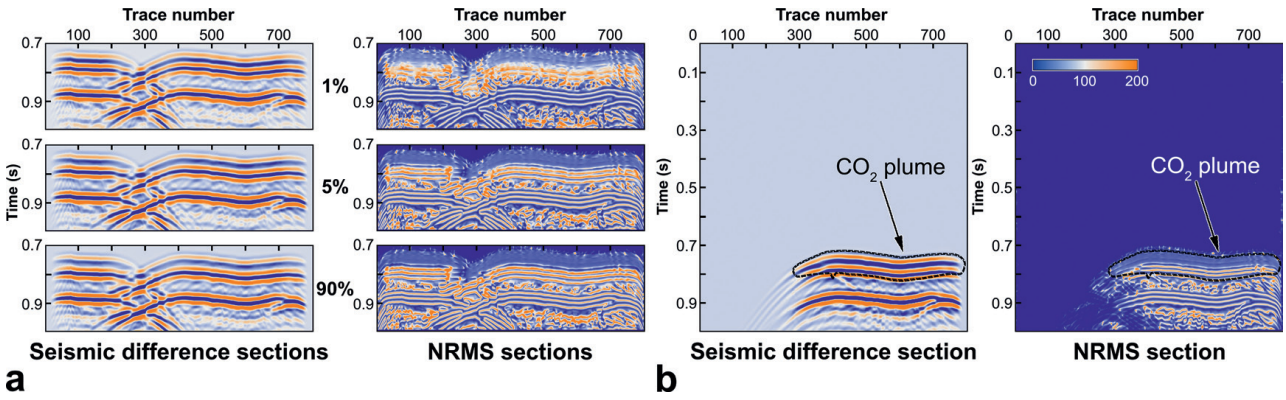

Fig. 6. Impact of petrophysical alteration on seismic sections. (**a**) The 'Difference' sections of the synthetic seismic lines of Scenario 1 (without petrophysical alteration) and Scenario 2 (with petrophysical alteration) with 1, 5 and 90% CO_2 saturation are presented in the left-hand plot. The corresponding NRMS sections are shown in the right-hand plot. Seismic sections of the reservoir and underlying rock are presented. (**b**) The 'Difference' section of the synthetic seismic lines of Scenario 3 and Scenario 4 (left-hand plot), and the corresponding NRMS section (right-hand plot); arrows indicate the CO_2 plume. The plume saturation model is shown in Figure 3.

saturation greater than 5%, the amplitude of the signals delineating the reservoir and the interface below did not vary significantly, similar to the reflection amplitudes of the reservoirs in the synthetic plane-wave sections.

Discussion

Analysis of the changes in the seismic response of the reservoir structure with different CO_2 saturation levels clearly revealed small quantities of CO_2 within the host formation in the E6 structure in seismic models. This phenomenon is due to a change in seismic velocities and quality factors, and consequently arrival times, and reflection amplitudes with an increasing CO_2 content from as little as 1% gas saturation. Therefore, the seismic monitoring of CO_2 injection within the considered E6 offshore structure is already effective from the very first steps of injection. Thus, the present research confirmed the results of previous studies, which suggested that accumulations of CO_2 as small as 500 tonnes (t) might be detectable under favourable conditions (Chadwick *et al*. 2006). Pawar *et al*. (2006) presented results from the West Pearl Queen pilot CO_2 injection project in SE New Mexico, which suggest that surface 3D seismics can detect 2090 t of CO_2 at a depth of 1372 m. But, at the same time, the results showed that the response of the West Pearl Queen reservoir during the field experiment was significantly different from the predicted response based on the pre-injection data. Numerical simulations with models based on the log analyses indicated that the West Pearl Queen reservoir is continuous between the injection well and the monitoring well, and that the response of CO_2 injection into the injection well would be observed in the monitoring well after about 6 months. However, the observed production response during the field experiment, as well as the geological interpretation based on the seismic data, imply that the reservoir is not continuous between the two wells. Pawar *et al*. (2006) also observed that the CO_2 injection rate was much lower than the estimates based on earlier characterization work. This indicates that the permeability of the reservoir to CO_2 injection is significantly different to the laboratory values measured on core samples prior to this project. According to Pawar *et al*. (2006), the latest numerical modelling algorithms do not capture the geochemical interactions, which are important elements in CGS modelling. In previous studies, we estimated and analysed petrophysical, geochemical and mineralogical alterations of the reservoir rocks from the studied E6 structure caused by laboratory simulated CO_2 storage (Shogenov *et al*. 2015*a*, *b*). Thus, in this paper, the alteration of petrophysical properties of reservoir rocks from the E6 offshore structure induced by CO_2–fluid–rock geochemical and mineralogical interactions during the modelled CO_2 storage were considered (Scenario 2 and Scenario 4). Nevertheless, for simplicity, in these two scenarios we implemented the results of the laboratory alteration experiment equally for all CO_2 saturation seismic sections, regardless of the actual CO_2 saturation values in the reservoirs.

The interfaces defining the three units forming the reservoir in the Cambrian Deimena Formation and the limestone oil reservoir in the Upper Ordovician Saldus Formation (Fig. 2) were impossible to distinguish on the baseline plane-wave seismic section due to the relatively low frequency of the modelled seismic source (35 Hz), which resulted in a single reflection.

The 'Difference' and NRMS sections of the layers overlying the reservoir rocks showed a zero amplitude for two-way travel times (TWT), which was less than those for the top of the reservoir reflection layer. In fact, the reflectors in this upper region of the seismogram were not influenced by the presence of CO_2, which changed the seismic characteristics of the later reflectors, identifying the top of the reservoir and the reflectors below (a greater TWT). This can be seen, for example, in Figure 5sc1-b, sc1-c.

The decrease in P-wave velocity due to the injected CO_2 caused the velocity push-down recognizable below the reservoir in all the synthetic seismic sections for all modelled scenarios. This phenomenon is well known and has already been documented in Arts *et al*. (2000), among others.

Previously published papers, based on theoretical (Domenico 1977; Jain 1987; Rossi *et al*. 2008; Picotti *et al*. 2012; Vera 2012) and field experimental (Arts *et al*. 2003, 2004*a*, *b*; Carcione *et al*. 2006; Chadwick *et al*. 2006) studies, reported a significant drop in the P-wave velocity values of sandy reservoir rocks at a CO_2 saturation of between 0 and 20%, and a slow increase after 30% CO_2 saturation. Laboratory studies of unconsolidated sands by Domenico (1974, 1976) show that the presence of gas reduces V_{Pwet} by as much as 30%, while V_{Swet} increases marginally (Jain 1987). Vera (2012) reported only 7% as a maximum change in V_{Pwet}. In our study, a 10–11% reduction in V_{Pwet} within 0–1% CO_2 saturation and a 20–22% decrease in V_{Pwet} after 5% CO_2 saturation were estimated (Tables 1–3). The V_{Swet} value did not increase significantly compared to V_{Pwet} (0.2–3%).

The trend of the acoustic impedance (i.e. the product of bulk density and the P-wave velocity) was strongly dominated by velocity. It showed an elbow point approximately where V_{Pwet} stopped decreasing and displayed a constant gentle decrease for increasing saturations (Fig. 4).

Table 2. *Estimated seismic (poro-viscoelastic) properties after the alteration experiment of the three reservoir layers of the Deimena Formation shown in the seismic model (Fig. 2)*

Layer	Lithology	ρ_{wet} (kg m^{-3})	φ (%)	κ (mD)	V_P (m s^{-1})	V_S (m s^{-1})	Q_P	Q_S	M (GPa)	K_{dry} (GPa)
Reservoir-1	Sandstone	2270	23	140	2743	1319	189	68	3.95	3.62
Reservoir-2	Sandstone	2388	16	90	2856	1283	1163	360	3.93	3.61
Reservoir-3	Sandstone	2188	30	280	2735	1415	202	81	4.38	4.01

All reservoir formations are saturated with brine.

Table 3. *Seismic properties of the reservoir layers of the Deimena Sandstone Formation partially saturated with CO_2*

			Initial*					Altered¶				
Layer	Fluid saturation		ρ_{wet} (kg m^{-3})	V_P (m s^{-1})	V_S (m s^{-1})	Q_P	Q_S	ρ_{wet} (kg m^{-3})	V_P (m s^{-1})	V_S (m s^{-1})	Q_P	Q_S
	Brine (%)	CO_2 (%)										
Reservoir-1	99	1	2340	2545	1411	127	52	2269	2443	1334	95	38
	95	5	2336	2262	1414	71	37	2264	2151	1337	52	27
	90	10	2331	2199	1412	93	51	2259	2084	1333	68	37
	85	15	2326	2172	1410	129	72	2253	2055	1331	94	53
	50	50	2291	2142	1416	>400	>400	2215	2023	1336	>400	>400
	10	90	2251	2152	1428	>400	>400	2171	2034	1349	>400	>400
Reservoir-2	99	1	2400	2581	1354	358	131	2387	2543	1286	>400	184
	95	5	2397	2236	1356	155	76	2384	2163	1288	219	104
	90	10	2393	2153	1356	187	99	2380	2069	1288	259	134
	85	15	2389	2116	1356	250	137	2377	2028	1288	341	184
	50	50	2362	2067	1361	>400	>400	2351	1972	1293	>400	>400
	10	90	2330	2069	1369	>400	>400	2321	1970	1301	>400	>400
Reservoir-3	99	1	2305	2644	1523	107	47	2187	2500	1427	102	45
	95	5	2300	2410	1527	61	33	2181	2266	1431	59	31
	90	10	2295	2356	1524	81	45	2174	2212	1429	78	43
	85	15	2288	2332	1523	113	65	2167	2189	1428	109	62
	50	50	2247	2311	1531	>400	>400	2118	2173	1439	>400	>400
	10	90	2200	2328	1546	>400	>400	2061	2195	1458	>400	>400

*Initial, before the alteration experiment (Figs 4 and 5sc1-a–sc1-c, sc3-a–sc3-c).
¶ Altered, after the alteration experiment (Figs 4 and 5sc2-a–sc2-c, sc4-a–sc4-c).

In our study, we consider plane-wave seismic simulations assuming normal or near-normal incidence. In this context, the reflection strength is proportional to the acoustic impedance contrast at different interfaces. The detectability of CO_2 by simple, direct comparison of seismograms depends on the variation in the acoustic impedance of the reservoir at increasing gas saturation. Acoustic impedance rapidly falls off for 0–5% CO_2 saturation, whereas the presence of this gas is revealed in seismograms, but decreases only slightly for higher saturation (Fig. 4c). This is due to the small P-wave velocity change with increasing CO_2 content (Fig. 4b). Consequently, variations in the reflection strength can barely be estimated for CO_2 saturations greater than 5%. It is likely to be more difficult to perform similar estimates for data complicated by realistic noise levels.

Converted shear modes can barely be produced in plane-wave simulations. Moreover, in this study we propose a conventional marine seismic survey where the pressure field is recorded just below the sea surface. S-wave velocity is slightly affected by the fluid substitution process and is basically not used in the analysis of seismic response. The shear-wave modulus must be known in order to compute the P-wave velocities of the storage aquifer, while S-wave velocities of the other formations are provided here for completeness. Parameters such as the V_P/V_S ratio are often used for fluid identification in reservoirs, and the S-wave field can be recorded at the seafloor by means of ocean-bottom seismometers or a permanent ocean-bottom cable system.

The quantitative estimation of CO_2 saturation from seismic data is beyond the scope of this study. However, the poor sensitivity of P-wave velocity to certain ranges of CO_2 saturation is a well-known phenomenon that should be considered in the use of seismic data for quantifying the gas content. In the velocity range weakly sensitive to variations in CO_2 saturation (above 10% in this study), the gas content can be quantified using additional geophysical methods. According to Eliasson *et al*. (2014), electrical conductivity is strongly dependent on gas saturation from 0 to 100%. Joint inversion of seismic and electromagnetic datasets has been proposed for estimating the relative amount of CO_2 with respect to brine (Eliasson *et al*. 2014; Böhm *et al*. 2015). The Amplitude Variation with Offset (AVO) technique for both P and PS converted waves can be used not only to determine the presence of CO_2 in the reservoir but also to estimate its saturation (e.g. Jin *et al*. 2000; Brown *et al*. 2007).

The time-lapse 'Difference' and NRMS section techniques supported the visualization of changes on the synthetic zero-offset seismic datasets and allowed monitoring of possible CO_2 plume evolution within the studied storage site. The comparison of synthetic seismic sections of two corresponding scenarios (Scenario 1 and Scenario 2, and Scenario 3 and Scenario 4) clearly showed the expected difference in signals for all CO_2 saturation levels (Fig. 6), proving the effectiveness of the implementation of the petrophysical alteration effect. Assuming that the laboratory-derived petrophysical changes are representative of a real reservoir, it may be possible to monitor the geochemical changes as well as the CO_2 saturation.

The ability to detect a 4D signal in field data depends both on the magnitude of the signal and on the noise level in the data. The synthetic dataset presented in this study is noise-free and represents an ideal seismic experiment to monitor CO_2 injection in the

E6 structure of the Baltic Sea. Unlike in real surveys, the repeatability of synthetic noise-free seismic data is optimal, and NRMS sections only highlight changes due to different reservoir conditions (i.e. the presence of CO_2). In marine seismic surveys, the repeatability ranges from 30% NRMS for streamer acquisitions with proper 4D data processing but significant mispositioning between surveys, down to 7% NRMS for acquisition using a permanent ocean-bottom cable system (Janssen *et al*. 2006). The best possible streamer repeatability is close to 10% NRMS (Brown & Paulsen 2011). We obtained the maximum NRMS values of 200% for panels sc1-c, sc2-c, sc3-c and sc4-c in Figure 5. When only considering NRMS values greater than 0.5, the arithmetic mean x_{NRMS} and the standard deviation σ_{NRMS} were: 83 and 64 for sc1-c; 108 and 67 for sc2-c; 100 and 77 for sc3-c; and 106 and 78 for sc4-c. We are confident that with a proper design for the time-lapse seismic survey and data-processing sequence, the level of 4D noise can be made sufficiently low and the NRMS metric will be able to reveal the presence of CO_2 in the Deimena Formation.

The above results show that the presented methodology can be proposed for modelling 4D monitoring and for assessing the reservoir integrity of CGS within the considered E6 structure. The methodology may also be extrapolated to storage sites with similar stratigraphy, lithology, and geochemical and petrophysical properties of rocks in the Baltic sedimentary basin, as well as in other geological basins. Electric and electromagnetic geophysical methods, and AVO analyses of P and PS converted waves, could be helpful in the quantitative estimation of CO_2 saturations in excess of 5–10%.

Conclusions

The main outcomes of this study can be summarized as follows:

- For the first time, seismic time-lapse numerical modelling based on rock physics studies was applied to monitor possible CO_2 storage in the largest geological structure, E6 offshore Latvia in the Baltic Sea.
- The novelty of the applied seismic numerical modelling approach was the coupling of the chemically induced petrophysical alteration effect of CO_2-hosting rocks measured in the laboratory with time-lapse numerical seismic modelling.
- Rock physics theories were applied to compute the petrophysical properties of the reservoir at different CO_2 saturations. Repeat synthetic seismic sections were produced and compared with the synthetic baseline section for four scenarios: (1) a uniform model without the alteration effect, (2) a uniform model with the alteration effect, (3) a plume model without the alteration effect; and (4) a plume model with the alteration effect.
- The presence of CO_2 in the Deimena Formation reservoir of Cambrian Series 3 in the E6 offshore structure could be inferred by direct interpretation of the synthetic plane-wave seismic sections, and more efficiently with 'Difference' and NRMS sections, through the time-lapse differences between the baseline and the repeat synthetic surveys.
- The effect of rock alteration due to the presence of CO_2 is clearly detectable on the 'Difference' and NRMS sections. It varied most of all on seismic sections with 1% CO_2 saturation, but decreased with an increase in CO_2 content.
- P-wave velocity decreased for the CO_2 saturation range 0−50%, with a steep drop in value between 0 and 5%, but increased slightly between 50 and 100% CO_2 saturation.
- The time-shift or push-down effect of reflectors below the CO_2 storage area was observed.
- This study, based on synthetic, noise-free datasets:
  - demonstrates the potential for the applied time-lapse rock physics and seismic methods to monitor the presence of the injected CO_2 within the considered E6 offshore oil-bearing structure from the beginning of CO_2 injection;
  - shows that, on the basis of changes in the amplitude and two-way travel times in the presence of CO_2, seismic surveys can detect CO_2 injected into deep aquifer formations, even with low CO_2 saturation values;
  - has significant importance for developing an optimal seismic monitoring plan in the study area and other areas with similar geological, lithological and petrophysical parameters.
- This study is based on scientifically validated rock physics theories and seismic numerical modelling codes, and intends to be a preliminary assessment of the seismic monitoring feasibility of geological storage of carbon dioxide in the Baltic area. Possible improvements of the methodology include shot-gather simulations with different levels of noise, and seismic processing to produce stack and migrated time-lapse synthetic sections. However, as for any other feasibility study, the effectiveness of seismic monitoring can be demonstrated only with a real time-lapse survey matching the modelled predictions.

Acknowledgements and Funding

This study was funded by EU FP7 Marie Curie Research Training Network 'Quantitative Estimation of Earth's Seismic Sources and Structure' (QUEST), Contract No. 238007, hosted by OGS (Trieste, Italy), Estonian targeted funding programmes (project IUT19-22) and is a part of K. Shogenov's PhD research. We would like to thank the editor of *Petroleum Geoscience*, anonymous reviewers and Daniel Sopher (Uppsala University) for useful comments and improvements to the paper.

References

Andrushenko, J., Vzosek, R. *et al*. 1985. *Report on the results of drilling and geological and geophysical studies in the exploration well E6-1/84*. Unpublished exploration report of E6-1/84 offshore well. Latvian Environmental, Geology and Meteorology Centre (LEGMC), Riga, Latvia (in Russian).

Arts, R., Brevik, I., Eiken, O., Sollie, R., Causse, E. & van der Meer, B. 2000. Geophysical methods for monitoring marine aquifer CO_2 storage – Sleipner experiences. *In*: Williams, D., Durie, B., McMullan, P., Paulson, C. & Smith, A. (eds) *Proceeding of the 5th International Conference on Greenhouse Control Technologies, Cairns*. CSIRO, Collingwood, Australia, 366–371, https://www.sintef.no/globalassets/project/ik23430000-sacs/publications/arts_et_al_ghgt5.pdf

Arts, R., Eiken, O., Chadwick, R.A., Zweigel, P., Van der Meer, L. & Zinszner, B. 2003. Monitoring of CO_2 injected at Sleipner using time lapse seismic data. *In*: Gale, J. & Kaya, Y. (eds) *Greenhouse Gas Control Technologies*. Elsevier, Oxford, 347–352.

Arts, R., Eiken, O., Chadwick, R.A., Zweigel, P., van der Meer, L. & Zinszner, B. 2004*a*. Monitoring of CO_2 injected at Sleipner using time-lapse seismic data. *In*: *Energy, 6th International Conference on Greenhouse Gas Control Technologies*, Elsevier, Oxford, **29**, 1383–1392.

Arts, R., Eiken, O., Chadwick, R.A., Zweigel, P., van der Meer, L. & Kirby, G.A. 2004*b*. Seismic monitoring at the Sleipner underground CO_2 storage site (North Sea). *In*: Baines, S. & Worden, R.J. (eds) *Geological Storage for CO2 Emissions Reduction*. Geological Society, London, Special Publications, **233**, 181–191, http://doi.org/10.1144/GSL.SP.2004.233.01.12

Arts, R., Chadwick, A., Eiken, O., Thibeau, S. & Nooner, S. 2008. Ten years of experience of monitoring CO_2 injection in the Utsira Sand at Sleipner, offshore Norway. *First Break*, **26**, 65–72.

Bachu, S., Bonijoly, D., Bradshaw, J., Burruss, R., Holloway, S., Christensen, N.P. & Mathiassen, O.M. 2007. CO_2 storage capacity estimation: Methodology and gaps. *International Journal of Greenhouse Gas Control*, **1**, 430–443.

Bacon, M., Simm, R. & Redshaw, T. 2003. *3-D Seismic Interpretation*. Cambridge University Press, Cambridge.

Batzle, M. & Wang, Z. 1992. Seismic properties of pore fluids. *Geophysics*, **57**, 1396–1408.

Bickle, M., Chadwick, A., Huppert, H.E., Hallworth, M. & Lyle, S. 2007. Modelling carbon dioxide accumulation at Sleipner: Implications for underground carbon storage. *Earth and Planetary Science Letters*, **255**, 164–176.

Boait, F., White, N., Bickle, M., Chadwick, R., Neufeld, J. & Huppert, H. 2012. Spatial and temporal evolution of injected CO_2 at the Sleipner field, North Sea. *Journal of Geophysical Research: Solid Earth*, **117**, 1978–2012.

Böhm, G., Carcione, J.M., Gei, D., Picotti, S. & Michelini, A. 2015. Cross-well seismic and electromagnetic tomography for CO_2 detection and monitoring in a saline aquifer. *Journal of Petroleum Science and Engineering*, **133**, 245–257.

Brocher, T.M. 2005. Empirical relations between elastic wave speeds and density in the Earth's crust. *Bulletin of the Seismological Society of America*, **95**, 2081–2092.

Brown, G. & Paulsen, J. 2011. Improved marine 4D repeatability using an automated vessel, source and receiver positioning system. *First Break*, **29**, 49–58.

Brown, S., Hagin, P. & Bussod, G. 2007. AVO monitoring of CO_2 sequestration. *SEG Technical Program Expanded Abstracts*, **2007**, 224–228, http://doi.org/10.1190/1.2792415

Carcione, J.M. 2007. *Wave Fields in Real Media: Wave Propagation in Anisotropic, Anelastic, Porous and Electromagnetic Media*, 2nd edition, revised and extended. Handbook of Geophysical Exploration: Seismic Exploration, **38**. Elsevier, Amsterdam.

Carcione, J.M., Helle, H.B. & Pham, N.H. 2003. White's model for wave propagation in partially saturated rocks: Comparison with poroelastic numerical experiments. *Geophysics*, **68**, 1389–1398.

Carcione, J.M., Picotti, S., Gei, D. & Rossi, G. 2006. Physics and seismic modeling for monitoring CO_2 storage. *Pure and Applied Geophysics*, **163**, 175–207.

Carcione, J.M., Gei, D., Picotti, S. & Michelini, A. 2012. Crosshole electromagnetic and seismic modeling for CO_2 detection and monitoring in a saline aquifer. *Journal of Petroleum Science and Engineering*, **100**, 162–172, http://doi.org/10.1016/j.petrol.2012.03.018

Castagna, J.P., Batzle, M.L. & Eastwood, R.L. 1985. Relationships between compressional-wave and shear-wave velocities in clastic silicate rocks. *Geophysics*, **50**, 571–581.

Castagna, J.P., Batzle, M. & Kan, T. 1993. Rock physics – The link between rock properties and AVO response. *In*: Castagna, J.P. & Backus, M. (eds) *Offset-Dependent Reflectivity – Theory and Practice of AVO Analysis*. Society of Exploration Geophysicists, Tulsa, OK, 135–171, http://www.gbv.de/dms/goettingen/583825389.pdf

Chadwick, A., Arts, R., Eiken, O., Williamson, P. & Williams, G. 2006. Geophysical monitoring of the CO_2 plume at Sleipner, North Sea: An outline review. *In*: Lombardi, S., Altunina, L.K. & Beaubien, S.E. (eds) *Advances in the Geological Storage of Carbon Dioxide: International Approaches to Reduce Anthropogenic Greenhouse Gas Emissions*. NATO Science Series IV: Earth and Environmental Sciences. Springer, Dordrecht, 303–314.

Chadwick, A., Arts, R., Bernstone, C., May, F., Thibeau, S. & Zweigel, P. 2008. *Best Practice for the Storage of CO2 in Saline Aquifers – Observations and Guidelines from the SACS and CO2STORE Projects, Volume 14*. British Geological Survey, Keyworth, Nottingham.

De Waals, J.A. 1986. *On the Rate Type Compaction Behaviour of Sandstone Reservoir Rock*. PhD thesis, Delft University of Technology, The Netherlands.

Domenico, S.N. 1974. Effect of water saturation on seismic reflectivity of sand reservoirs encased in shale. *Geophysics*, **39**, 759–769.

Domenico, S.N. 1976. Effect of brine-gas mixture on velocity in an unconsolidated sand reservoir. *Geophysics*, **41**, 882–894.

Domenico, S.N. 1977. Elastic properties of unconsolidated porous sand reservoirs. *Geophysics*, **42**, 1339–1368.

Dortman, N.B. (ed.). 1992. *Petrophysics. A Handbook. Book 1. Rocks and Minerals*. Nedra, Moscow (in Russian).

Eliasson, P., Romdhane, A., Jordan, M. & Querendez, E. 2014. A synthetic Sleipner study of CO_2 quantification using controlled source electro-magnetics and full waveform inversion. *Energy Procedia*, **63**, 4249–4263, http://doi.org/10.1016/j.egypro.2014.11.460

Fornel, A. & Estublier, A. 2013. To a dynamic update of the Sleipner CO_2 storage geological model using 4D seismic data. *Energy Procedia*, **37**, 4902–4909, http://doi.org/10.1016/j.egypro.2013.06.401

Gardner, G.H.F., Gardner, L.W. & Gregory, A.R. 1974. Formation velocity and density – The diagnostic basics for stratigraphic traps. *Geophysics*, **39**, 770–780.

Gercek, H. 2007. Poisson's ratio values for rocks. *International Journal of Rock Mechanics and Mining Sciences*, **44**, 1–13.

Gregory, A.R. 1977. Fluid saturation effects on dynamic elastic properties of sedimentary rocks. *Geophysics*, **41**, 895–921.

Grigelis, A. 2011. Research of the bedrock geology of the Central Baltic Sea. *Baltica*, **24**, 1–12.

Haase, A. & Stewart, R. 2004. Attenuation estimates from VSP and log data. *In*: *74th Annual International Meeting, SEG Expanded Abstracts*. Society of Exploration Geophysicists, Tulsa, OK, 2497–2500.

Holloway, S. 2005. Underground sequestration of carbon dioxide – a viable greenhouse gas mitigation option. *Energy*, **30**, 2318–2333.

Huppert, H.E. & Woods, A.W. 1995. Gravity-driven flows in porous layers. *Journal of Fluid Mechanics*, **292**, 55–69.

IEA. 2004. *Prospects for CO_2 Capture and Storage*. IEA (International Energy Agency)/OECD, Paris.

IEA. 2013. *CO_2 Emissions from Fuel Combustion*. Highlights. IEA (International Energy Agency)/OECD, Paris.

IPCC. 2005. Metz, B., Davidson, O., de Coninck, H.C., Loos, M. & Meyer, L.A. (eds) *IPCC Special Report on Carbon Dioxide Capture and Storage. Prepared by Working Group III of the Intergovernmental Panel on Climate Change*. Cambridge University Press, Cambridge.

IPCC. 2013. *Working Group I Contribution to the IPCC Fifth Assessment Report, Climate Change 2013: The Physical Science Basis, Summary for Policy Makers*. IPCC (Intergovernmental Panel on Climate Change), Geneva, http://www.climatechange2013.org

Jain, S. 1987. Amplitude-vs-offset analysis: A review with references to application in western Canada. *Canadian Society of Exploration Geophysicists Journal*, **23**, 27–36.

Janssen, A., Byerley, G., Ediriweera, K., Hope, T., Rasmussen, K. & Westeng, K. 2006. Simulation-driven seismic modeling applied to the design of a reservoir surveillance system for Ekofisk Field. *The Leading Edge*, **25**, 1176–1185.

Jin, S., Cambois, G. & Vuillermoz, C. 2000. Shear-wave velocity and density estimation from PS-wave AVO analysis: Application to an OBS dataset from the North Sea. *Geophysics*, **65**, 1446–1454.

Kazemeini, S.H., Juhlin, C. & Fomel, S. 2010. Monitoring CO_2 response on surface seismic data; a rock physics and seismic modeling feasibility study at the CO_2 sequestration site, Ketzin, Germany. *Journal of Applied Geophysics*, **71**, 109–124.

Kragh, E. & Christie, P. 2002. Seismic repeatability, normalized RMS, and predictability. Society of Exploration Geophysicists. *The Leading Edge*, **21**, 640–647.

Lacombe, C.H., Campbell, S. & White, S. 2011. Improvements in 4D seismic processing – Foinaven 4 years on. Extended Abstract. Paper presented at the *73rd EAGE Conference & Exhibition incorporating SPE EUROPEC 2011*, 23−26 May 2011, Vienna, Austria.

Ludwig, W.J., Nafe, J.E. & Drake, C.L. 1970. Seismic refraction. *In*: Maxwell, A.E. (ed.) *The Sea, Volume 4*. Wiley–Interscience, New York, 53–84.

Lyle, S., Huppert, H.E., Hallworth, M., Bickle, M. & Chadwick, A. 2005. Axisymmetric gravity currents in a porous medium. *Journal of Fluid Mechanics*, **543**, 293–302.

MacBeth, C., Stammeijer, J. & Omerod, M. 2006. Seismic monitoring of pressure depletion evaluated for a United Kingdom continental-shelf gas reservoir. *Geophysical Prospecting*, **54**, 29–47.

National Research Council. 2010. *Ocean Acidification: A National Strategy to Meet the Challenges of a Changing Ocean*. The National Academies Press, Washington, DC.

Pawar, R.J., Warpinski, N.R. *et al* 2006. Overview of a CO_2 sequestration field test in the West Pearl Queen reservoir, New Mexico. *Environmental Geosciences*, **13**, 163–180.

Peng, D.Y. & Robinson, D.B. 1976. A new two-constant equation of state. *Industrial & Engineering Chemistry Fundamentals*, **15**, 59–64.

Picotti, S., Carcione, J.M., Gei, D., Rossi, G. & Santos, J.E. 2012. Seismic modeling to monitor CO_2 geological storage: The Atzbach-Schwanenstadt gas field. *Journal of Geophysical Research*, **117**, B06103, http://doi.org/10.1029/2011JB008540

Rossi, G., Gei, D., Picotti, S. & Carcione, J.M. 2008. CO_2 storage at the Aztbach-Schwanenstadt gas field: A seismic monitoring feasibility study. *First Break*, **26**, 45–51.

Saxena, V. 2004. Role of associated minerals and porosity in VP–VS response for sandstone and limestone. Paper presented at the *International Symposium of the Society of Core Analysts*, Abu Dhabi, UAE, 5–9 October 2004, SCA2004–46, 1–7, http://www.ux.uis.no/~s-skj/ipt/Proceedings/SCA.1987-2004/1-SCA2004-46.pdf

Shogenov, K. & Gei, D. 2013. Seismic numerical modeling to monitor CO_2 storage in the Baltic Sea offshore structure. *In*: *74th EAGE Conference & Exhibition incorporating SPE EUROPEC 2013*, *10–13 June 2013*, *London, UK*. European Association of Geoscientists and Engineers (EAGE), Houten, The Netherlands, 1–4.

Shogenov, K., Shogenova, A. & Vizika-Kavvadias, O. 2013*a*. Petrophysical properties and capacity of prospective structures for geological storage of CO_2 onshore and offshore Baltic. *Energy Procedia*, **37**, 5036–5045, http://doi.org/10.1016/j.egypro.2013.06.417

Shogenov, K., Shogenova, A. & Vizika-Kavvadias, O. 2013*b*. Potential structures for CO_2 geological storage in the Baltic Sea: Case study offshore Latvia. *Bulletin of the Geological Society of Finland*, **85**, 65–81.

Shogenov, K., Shogenova, A., Vizika-Kavvadias, O. & Nauroy, J.F. 2015*a*. Experimental modeling of CO_2–fluid–rock interaction: The evolution of the composition and properties of host rocks in the Baltic Region. *Earth and Space Science*, **2**, 262–284.

Shogenov, K., Shogenova, A., Vizika-Kavvadias, O. & Nauroy, J.F. 2015*b*. Reservoir quality and petrophysical properties of Cambrian sandstones and their changes during the experimental modelling of CO_2 storage in the Baltic Basin. *Estonian Journal of Earth Science*, **64**, 199–217.

Shogenova, A., Sliaupa, S., Vaher, R., Shogenov, K. & Pomeranceva, R. 2009*a*. The Baltic Basin: Structure, properties of reservoir rocks and capacity for geological storage of CO_2. Tallinn. Estonian Academy Publishers. *Estonian Journal of Earth Sciences*, **58**, 259–267.

Shogenova, A., Šliaupa, S. *et al*. 2009*b*. Possibilities for geological storage and mineral trapping of industrial CO_2 emissions in the Baltic region. *Energy Procedia*, **1**, 2753–2760.

Shogenova, A., Kleesment, A., Shogenov, K., Põldvere, A. & Jõeleht, A. 2010. Composition and properties of Estonian Palaeozoic and Ediacaran sedimentary rocks. *In*: *72nd EAGE Conference & Exhibition incorporating SPE EUROPEC 2010*, *14–17 June 2010*, *Barcelona*, pp1-5. European Association of Geoscientists and Engineers (EAGE), Houten, The Netherlands.

Shogenova, A., Shogenov, K. *et al*. 2011*a*. CO_2 geological storage capacity analysis in Estonia and neighboring regions. *Energy Procedia*, **4**, 2785–2792.

Shogenova, A., Shogenov, K., Pomeranceva, R., Nulle, I., Neele, F. & Hendriks, C. 2011*b*. Economic modelling of the capture–transport–sink scenario of industrial CO_2 emissions: The Estonian–Latvian cross-border case study. *Energy Procedia*, **4**, 2385–2392.

Sliaupa, S., Shogenova, A., Shogenov, K., Sliaupiene, R., Zabele, A. & Vaher, R. 2008. Industrial carbon dioxide emissions and potential geological sinks in the Baltic States. *Oil Shale*, **25**, 465–484.

Šliaupa, S., Lojka, R. *et al*. 2013. CO_2 storage potential of sedimentary basins of Slovakia, the Czech Republic, Poland, and Baltic States. *Geological Quarterly*, **57**, 219–232.

Vedanti, N., Pathak, A., Srivastava, R.P. & Dimri, V.P. 2009. Time lapse (4D) seismic: Some case studies. *e-Journal Earth Science India*, **4**, 230–248, http://www.earthscienceindia.info/pdfupload/download.php?file=tech_pdf-1292.pdf

Vera, C.V. 2012. *Seismic modelling of CO_2 in a sandstone aquifer*. MSc thesis, University of Calgary, Alberta, http://hdl.handle.net/1880/48934

Udias, A. 1999. *Principles of Seismology*. Cambridge University Press, Cambridge.

USEPA. 2013. *Causes of Climate Change*. United States Environmental Protection Agency, Washington, DC, http://www.epa.gov/climatechange/science/causes.html last accessed February 22, 2013

United States Geological Survey Geologic Carbon Dioxide Storage Resources Assessment Team. 2013. *National Assessment of Geologic Carbon Dioxide Storage Resources. Results*. United States Geological Survey Circular, **1386**, 41, http://pubs.usgs.gov/circ/1386

Waters, K. 1978. *Reflection Seismology. A Tool for Energy Resource Exploration*. Wiley, New York.

White, J.E. 1965. *Seismic Waves: Radiation, Transmission and Attenuation*. McGraw-Hill, New York.

White, J.E. 1975. Computed seismic speeds and attenuation in rocks with partial gas saturation. *Geophysics*, **40**, 224–232.

Zhang, Z. & Agarwal, R. 2014. Numerical simulation and optimization of Sleipner carbon sequestration project. *International Journal of Engineering & Technology*, **3**, 1–13, http://doi.org/10.14419/ijet.v3i1.1439